PROCEEDINGS OF THE INTERNATIONAL CONFERENCE
NANOMATERIALS: APPLICATIONS AND PROPERTIES
Vol. **2** No 2, 02FNC27(3pp) (2013)

Obtaining of TiN/MoN Nanocomposite Coatings and Their Research

A.D. Pogrebnjak[1], G. Abadias[2], O.V. Bondar[1], B.O. Postolnyi[1,*], A.A. Andreev[3], V.M. Beresnev[4],
P. Chartier[2], O.V. Sobol[5], O. Maksakova[1]

[1] *Sumy State University, 2, Rymskogo-Korsakova st., Sumy, 40007, Ukraine*
[2] *Institute Pprime, University of Poitiers, 15, Rue de l'Hôtel Dieu, Poitiers Cedex, Poitiers, 86022, France*
[3] *National Science Center «KIPT», 1, Akademicheskaya St., Kharkiv, 61108, Ukraine*
[4] *V.N. Karazin Kharkiv National University, 6, Svobody sq., Kharkiv, 61022, Ukraine*
[5] *National Technical University «Kharkiv Polytechnic Institute», 21, Frunze str., Kharkiv, 61002, Ukraine*

(Received 06 August 2013; published online 01 September 2013)

At the nanometer scale multilayer nanostructured coatings show special properties due to the depositions conditions. This paper presents results of TiN/MoN nanocomposites obtaining and their research. Multilayer coatings based on TiN/MoN were deposited using vacuum arc evaporation cathode method (C-PVD). Total thickness range of obtained coatings was 2, 10, 20 and 40 nm. We used vacuum-arc device "Bulat-6" for coatings deposition. Structure and properties of multilayer coatings were analyzed using XRD (Bruker D-8 Advance) in Cu-K_α radiation, high resolution transmission electron microscopy (HRTEM system) with diffraction CFEI EO Techai F200, SEM with EDX (JEOL-7001F). Scratch tests were carried out using Rockwell-C diamond indenter (CSM Revetest Instruments) with a tip radius of 200 µm. Besides this, ball-on-plate sliding test on UMT-3MT tribometer (CETR, USA) was used for additional investigation of friction and wear.

This research allowed to reveal structural and properties depending on deposition conditions of TiN/MoN multilayer coatings. The nanocomposite hardness value increases when monolayer thickness decreases. This also reduced nanograins size. Measurement of the friction coefficient demonstrates smaller values for multilayer system in comparison with TiN or MoN nanostructured coatings. Formation of a (Ti, Mo)N solid solution and nanocrystals growing were observed during annealing.

Keywords: Nanocomposites, Nitrides, Biphasic, Wear, Hardness, Interphase boundary, Deposition, Multilayer.

PACS numbers: 61.46. – w. 62.20.Qp, 62.25. – q.

1. INTRODUCTION

Nowadays, the study of nanocomposite materials causes a great interest of academics and industry. This is due to the special properties which materials demonstrate at nanosize level because of small grains size (less than 10 nm) and greater importance of the boundary zones [1-3]. It is known that hardness of Mo coatings is $32 \div 55$ GPa and their deposition on cutting tools greatly increases wear resistance [4]. At the same time, TiN coatings have hardness 32 GPa and in individual cases hardness rises up to 40 GPa or higher [2, 5]. It's also known that Ti-Mo-N multilayer coatings show 2-4 times durability increasing in comparison with conventional coatings based on TiN [6-8].

Structure and properties of TiN/MoN nanocomposites, their dependence on the monolayer thickness were investigated in this article.

2. DESCRIPTION OF NANOCOMPOSITE DEPOSITION AND INVESTIGATION

Multilayer nanostructured TiN/MoN coatings were obtained using vacuum-arc device "Bulat-6". A scheme of this device showed on Fig. 1. Thickness of deposited nanosized monolayers (TiN and MoN) was about 2, 10, 20, 40 nm and total thickness was in the range from 6.8 to 8.2 µm.

Deposition of titanium and molybdenum nitrides starts after the nitrogen injection into the chamber. When first layers have been finished, deposition stops and substrates turn over on the angle of 180°. Then deposition starts again.

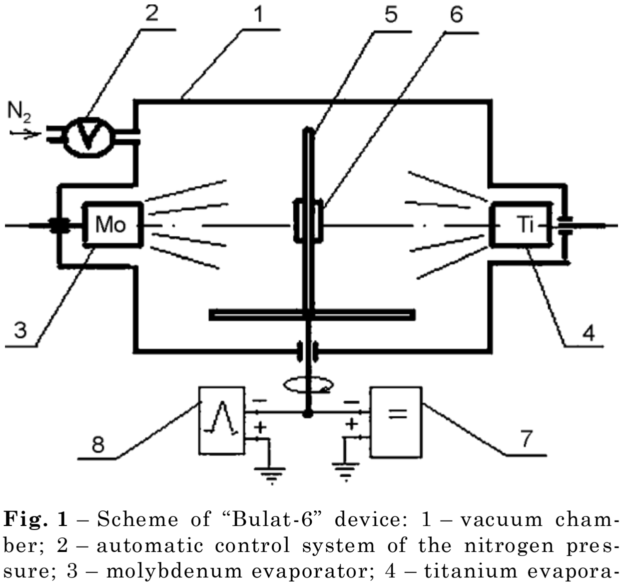

Fig. 1 – Scheme of "Bulat-6" device: 1 – vacuum chamber; 2 – automatic control system of the nitrogen pressure; 3 – molybdenum evaporator; 4 – titanium evaporator; 5 – substrate holder; 6 – substrate; 7 – DC voltage source; 8 – high voltage impulse generator

---

*b.postolnyi@gmail.com

Rutherford backscattering (RBS) on He$^+$ ions with energy 1.7 MeV was used to obtain information about elemental structure (scattering angle θ = 170° at normal probing ions falling, detector energy resolution was 16 keV, helium ions dose was 5 μm).

Investigation of coatings microstructure and element composition was carried out using JEOL-7001F with microanalysis EDX (Japan) and other scanning electron-ion microscopes. Coatings structure and phase composition were analyzed using XRD (Bruker Advanced 8) in Cu-K$_\alpha$ radiation.

Hardness and elastic modulus measurement were carried out with CSM company device (Switzerland). Phase composition analysis was performed using ASTM catalogs.

3. RESULTS AND DISCUSSION

There is only one phase with FCC lattice (structural type NaCl) formed in coating at a low substrate potential 40 V at monolayer thickness nearby 2 nm. Diffraction patterns showed on Fig. 2. When substrate potential increased to -230 V it causes formation of two-phase TiN system and high-temperature γ-Mo_2N with phase ratio TiN/MoN equal to 90/10 respectively. The appearance of a two-phase condition is an intensive ion bombardment which promotes nanograins grinding and interfaces formation. This is accompanied by separate Mo_2N layers with cubic lattice and interface formation. In turn, it leads to stress growing in the TiN phase and period increasing in tense cross-section. In this case layers structure is columnar.

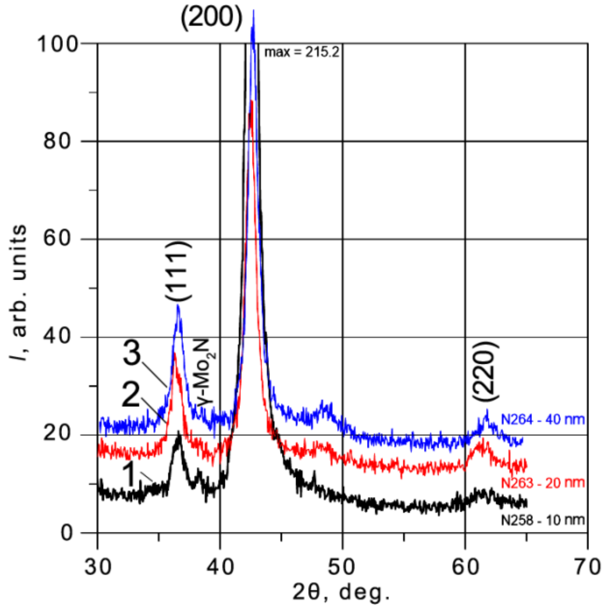

Fig. 2 – Fragments of the diffraction patterns (XRD), obtained for coating samples with monolayer thickness 10, 20, 40 nm

Formation of the two-phase structural state with an average TiN and γ-Mo_2N cubic phase grade 60 vol.% and 40 vol.% occurs when monolayers thickness increase to 10 nm. These values are close to Ti and Mo concentrations (62.3 at.% and 36.8 at.% respectively, see Fig. 3), which were obtained by EDX.

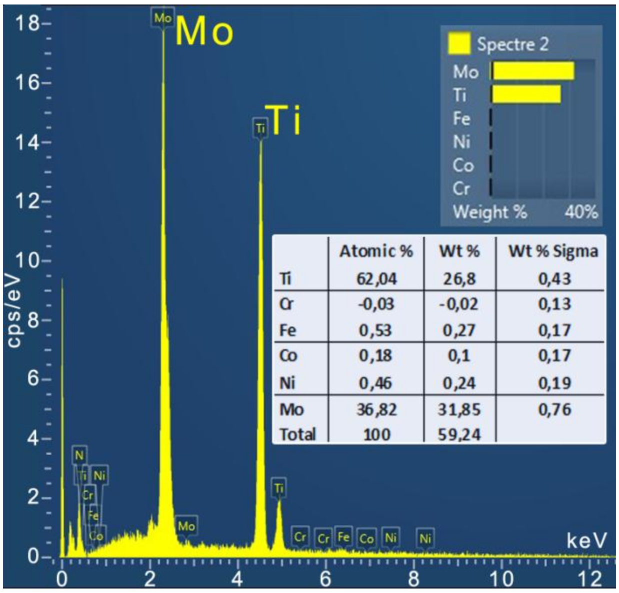

	Atomic %	Wt %	Wt % Sigma
Ti	62,04	26,8	0,43
Cr	-0,03	-0,02	0,13
Fe	0,53	0,27	0,17
Co	0,18	0,1	0,17
Ni	0,46	0,24	0,19
Mo	36,82	31,85	0,76
Total	100	59,24	

Fig. 3 – The energy-dispersive spectrum, obtained on multilayer nanocomposite coating with monolayer thickness 20 nm

The full cross-section of nanostructured coatings is presented on the next figure (Fig. 4). Fig. 5 shows striped TiN nanosized layers – dark areas and MoN – light areas which are well recognizable at this zoom.

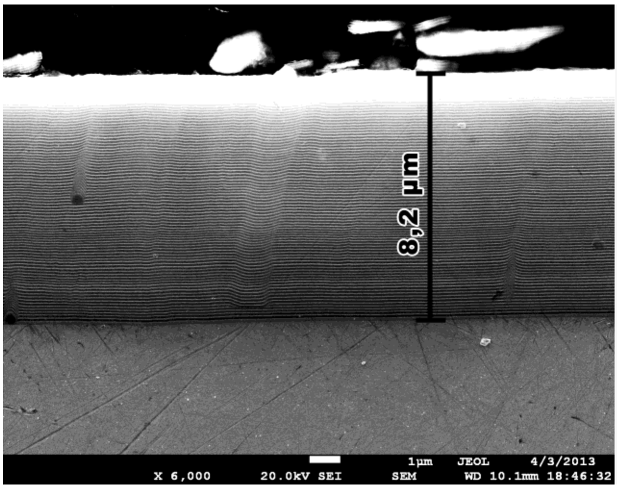

Fig. 4 – The microphotograph of cross-sections of nanostuctured multilayer Ti-Mo-N coating. The general view. The coating thickness is 8.2 μm

The appearance of interface specific volume caused by high γ-Mo_2N phase level is accompanied by high γ-Mo_2N phase level is accompanied by high compressive stress growth in titanium nitride, it achieved maximum hardness 32 GPa (Fig. 6).

Noteworthy that only γ-Mo_2N phase presents in molybdenum nitride and no β-Mo_2N phase is formed, although both of them can be formed in case of vacuum-arc deposition. This can be explained by two-stage phase composition of multilayered nanostructured coating. At the initial growth of Mo_2N the determining factor is TiN lattice atomic sequence.

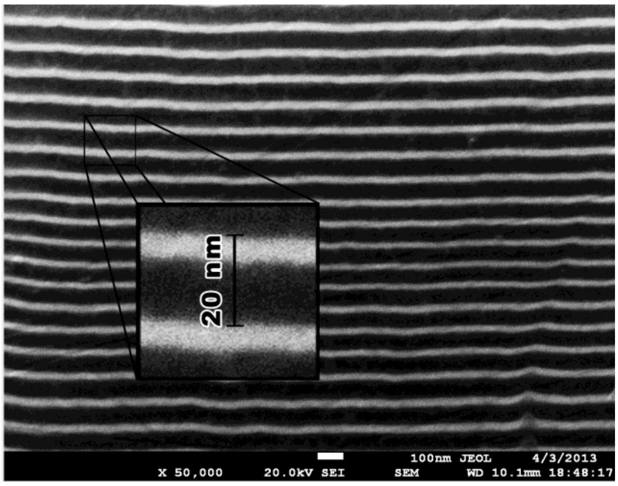

Fig. 5 – The microphotograph of cross-sections of nanostuctured multilayer Ti-Mo-N coating. The cross-section fragment,× 50 000 zoom. The monolayer thickness is 20 nm

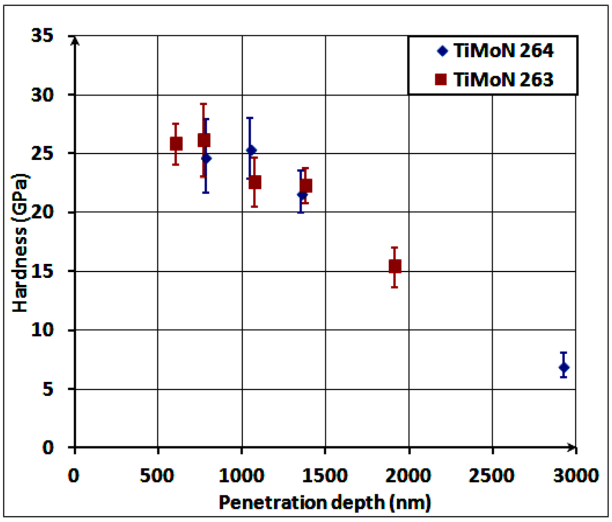

Fig. 6 – The micro-hardness characteristics: a) The dependence on the indenter penetration depth of microhardness H at monolayers thickness 20 and 40 nm

Therefore, there is a γ-Mo_2N cubic modification stabilization with molybdenum nitride layer growing. This is accompanied by a macrodeformation resetting and interface formation caused by structured macrostress when relatively high thickness. Volume content of the phases accurately corresponds to the expected in according to the EDX analysis (70 at.% TiN and 30 at.%) for samples with coating thickness nearby 20 nm. Monolayer thickness increasing up to 40 nm leads to Mo_2N fraction increasing up to 40%. At the same time hardness has the lowest value (not greater than 26 GPa).

4. CONCLUSIONS

The tribological properties analysis shows that surface roughness Ra reaches the value 0.3 μm, friction coefficient varies from 0.09 to 0.12. Critical load (when coating starts to break) ranges from 425 N at monolayer thickness 40 nm, and reaches (610 ÷ 648) N at thickness 10 and 2 nm. Thus, the less monolayer thickness, the higher load. This shows that one nitride monolayer envelops nanograins in the last case. Therefore, nanocomposite strength increases by grains shift prevention (slipping). According to Koehler's model [8] the possible mechanism of hardness increasing is transfer of valence charge, reduction nanograins size and mixing entropy.

The smallest wear was observed under deposition conditions for monolayers thickness 2 and 10 nm, equals 0.148 for counterbody and 2.327×10^{5} [mm^{3}·N^{1}·mm^{-1}] for coating. Samples annealing during 2 hours at temperature 800 °C in an oven under vacuum 10 – 2 Pa causes reducing of compressive stress and small nanograins growth to 10 ÷ 15 % (no more).

ACKNOWLEDGEMENTS

The work was performed within the framework of scientific-technical cooperation program with the University of Poitiers, as well as comprehensive state program “Development of the basis for formation of multicomponent nanostructured superhard coatings with high physical and mechanical properties” (number 0112U001382) and “Physical principles of plasma technologies for complex processing of multicomponent materials and coatings” (number 0113U000137).

REFERENCES

1. A.D. Pogrebnjak, A.P. Shpak, N.A. Azarenkov, V.M. Beresnev, *Phys. Usp.* **52**, 29 (2009).
2. M.K. Kazmanli, M. Urgen, A.F. Cakir, *Surf. and Coat. Tech.* **167**, 77 (2003).
3. A.D. Pogrebnjak, A.G. Ponomarev, A.P. Shpak, Yu.A. Kunitskii, *Phys. Usp.* **55**, 270 (2012);
4. A.D. Pogrebnyak, V.M. Beresnev, A.Sh. Kaverina, A.P. Shypylenko, O.V. Kolisnichenko, K. Oyoshi, Y. Takeda, H. Murakami, D.A. Kolesnikov, M.S. Prozorova, *Tech. Phys. Lett.* **39**, 189 (2013).
5. A.D. Pogrebnjak, A.P. Shpak, V.M. Beresnev, D.A. Kolesnikov, Yu.A. Kunitskii, O.V. Sobol, V.V. Uglov, F.F. Komarov, A.P. Shypylenko, N.A. Makhmudov, A.A. Demyanenko, V.S. Baidak, V.V. Grudnitskii, *Journal of Nanoscience and Nanotechnology* **12**, 9213 (2012).
6. R. Krause-Rehberg, A.D. Pogrebnjak, V.N. Borisyuk, M.V. Kaverin, A.G. Ponomarev, M.O. Bilokur, K. Oyoshi, Y. Takeda, V.M. Beresnev, O.V. Sobol, *The Physics of Metals and Metallography* **114,** 731 (2013).
7. A.D. Pogrebnjak, V.M. Beresnev, A.A. Demianenko, V.S. Baidak, F.F. Komarov, M.V. Kaverin, N.A. Makhmudov, D.A. Kolesnikov, *Phys. Solid State* **54**, 1882 (2012).
8. V. Ivashchenko, S. Veprek, A.D. Pogrebnjak, *Proceedings of the International Conference Nanomaterials: Applications and Properties* **1**, 03PCSI19 (2012).